Energetic ion precipitation at Titan

T. E. Cravens,[1] I. P. Robertson,[1] S. A. Ledvina,[2] D. Mitchell,[3] S. M. Krimigis,[3,4] and J. H. Waite Jr.[5]

Received 25 October 2007; revised 7 December 2007; accepted 28 December 2007; published 6 February 2008.

[1] Energetic protons and oxygen ions have been observed in Saturn's outer magnetosphere and can precipitate into Titan's atmosphere where they deposit energy, ionize, and drive ionospheric chemistry. Ion production rates caused by this precipitation are calculated using fluxes of incident 27 keV to 4 MeV protons measured by the Cassini MIMI instrument. We find that significant ion production rates exist in the 500 km to 1000 km altitude range and estimate associated electron densities of about 200–2000 cm^{-3} in reasonable agreement with measured densities. We demonstrate that energetic oxygen ions do not penetrate below about 650 km, but they can also generate significant ionization. We suggest that a few percent of the oxygen flux is converted to negative O ions as a consequence of charge exchange collisions, which might help explain the negative ions observed near 960 km by the Cassini CAPS instrument. **Citation:** Cravens, T. E., I. P. Robertson, S. A. Ledvina, D. Mitchell, S. M. Krimigis, and J. H. Waite Jr. (2008), Energetic ion precipitation at Titan, *Geophys. Res. Lett.*, *35*, L03103, doi:10.1029/2007GL032451.

1. Introduction

[2] Titan is Saturn's largest satellite and it has a dense atmosphere composed of molecular nitrogen and methane, with minor amounts of many hydrocarbon and nitrile species [*Waite et al.*, 2005]. Solar radiation and energetic plasma from Saturn's magnetosphere ionize the neutral atmosphere and create an ionosphere at altitudes above about 800 km [*Bird et al.*, 1997; *Wahlund et al.*, 2005; *Cravens et al.*, 2005]. Ionospheric layers near 600 km due to meteor ablation were also suggested [*Molina-Cuberos et al.*, 2001]. The Cassini Radio Science Experiment recently observed an intermittent (about half the time) ionospheric layer with substantial electron densities ($n_e \approx 200–2000\ cm^{-3}$) between 500 km and 900 km (A. J. Kliore et al., First results from the Cassini radio occultations of the Titan ionosphere, submitted to *Journal of Geophysical Research*, 2007, hereinafter referred to as Kliore et al., submitted manuscript, 2007). The Voyager radio occultation experiment might also have seen an ionosphere at very low altitudes [*Bird et al.*, 1997]. The creation of an ionosphere below 1000 km by precipitating magnetospheric electrons requires substantial fluxes of electrons with energies in excess of 1 keV [cf. *Gan et al.*, 1992; *Agren et al.*, 2007], but this is very sensitive to magnetic field topology.

[3] Several keV ions mostly charge transfer with neutrals, creating fast neutrals at altitudes well above 1000 km [*Michael et al.*, 2005]. Precipitation of such ions can result in atmospheric loss via sputtering processes [*Michael et al.*, 2005]. *Luna et al.* [2003] studied ionization by more energetic magnetospheric ions for altitudes above 1000 km. Using magnetospheric fluxes of protons and oxygen ions from the Voyager and Cassini missions, we describe in the current paper how the precipitation of energetic ions can create an ionosphere below 1000 km. We also suggest that some precipitating oxygen atoms can acquire an electron (becoming O^- ions) and that these ions then transfer electrons to atmospheric species such as NH_3 or CH_4, thus initiating atmospheric negative ion chemistry which might help to explain Cassini observations of negative ions near 960 km [*Coates et al.*, 2007a].

2. Energetic Ions in Saturn's Outer Magnetosphere

[4] The Voyager PLS experiment observed in the outer magnetosphere both protons and a higher mass species (N^+ was suggested but now this is known to be O^+ [*Hartle et al.*, 2006]). The ions (densities $\approx 0.1–0.2\ cm^{-3}$) were drifting in the co-rotation direction at about 120 km/s and had comparable "thermal" speeds [see *Neubauer et al.*, 1984; *Hartle et al.*, 2006]. Average proton and heavy ion energies found by PLS were a few hundred eV (protons) and a few keV (heavies), respectively. The CAPS and MIMI instruments onboard Cassini also measured energetic ions in the outer magnetosphere [*Young et al.*, 2005; *Krimigis et al.*, 2005]. The LEMMS sensor on the MIMI experiment measured 27 keV–4 MeV ion fluxes that showed considerable variability. Two overall situations are evident: higher fluxes when the spacecraft is in the current sheet (e.g., the T5 Cassini encounter with Titan), and lower fluxes outside the current sheet (a more "typical" situation). We use the T5 MIMI measurements for the high flux scenario and we also extract a typical low flux spectrum from the MIMI dataset (see Figure 1). Figure 1 also shows total ion fluxes for energies less than ≈10 keV consistent with Voyager data. We simply interpolated between the few keV PLS observations and the higher energy MIMI data with a power law.

[5] We make two extreme assumptions about energetic ion composition – that the incident ions are either all protons or are all oxygen. The composition issue will need to be revisited when more data have been analyzed. Particle spectra are represented in our codes using a number of

[1]Department of Physics and Astronomy, University of Kansas, Lawrence, Kansas, USA.
[2]Space Science Laboratory, University of California, Berkeley, California, USA.
[3]Applied Physics Laboratory, Johns Hopkins University, Laurel, Maryland, USA.
[4]Also at Academy of Athens, Athens, Greece.
[5]Southwest Research Institute, San Antonio, Texas, USA.

0094-8276/08/2007GL032451

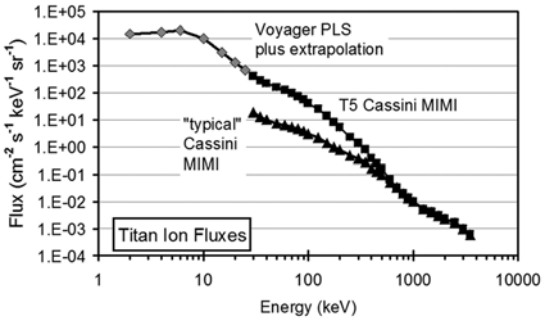

Figure 1. Differential ion flux versus particle energy for protons as measured by the Cassini LEMMS experiment for the time period 2005 106 19:00:00–2005 106 19:10:00 (outer magnetosphere of Saturn for T5 Titan pass). The same spectrum was adopted for oxygen above 27 keV. The lower energy oxygen spectrum used in our calculations was derived from Voyager data plus an interpolation to energies up to 27 keV. Also shown is a typical lower flux spectrum from the Cassini MIMI experiment.

"beams" −32 for protons with energies between 27 keV and 4 MeV and 36 for oxygen (2 keV–4 MeV).

[6] Saturn's magnetic field drapes around Titan forming a magnetic barrier and a magnetotail [e.g., *Neubauer et al.*, 1984; *Backes et al.*, 2005; *Ledvina and Cravens*, 1998; *Ma et al.*, 2004] shielding Titan from lower energy protons but not from heavy ions [see *Ledvina et al.*, 2005]. Induced magnetic fields near Titan at roughly B ≈ 10–15 nT are about double the external magnetospheric field. Shielding effectiveness can be roughly estimated using ion gyroradii. The gyroradius (r_g) in units of Titan radii (R_T) for B = 10 nT is given by: $r_g \approx 0.17\ (E\ m)^{1/2}$, where E is ion energy in keV and m is ion mass in amu. The gyroradius is smaller than Titan ($r_g \approx 0.1\ R_T$) and magnetic shielding is effective for thermal protons but not for colder (3 keV) thermal heavy ions ($r_g \approx 1\ R_T$). For protons, r_g exceeds unity only for E > 30 keV and we simply adopt 30 keV as a shielding cut-off. A paper describing a numerical simulation of shielding effects is in preparation by S. A. Ledvina et al.

3. Energetic Oxygen and Proton Precipitation at Titan

[7] Neutral atmospheric densities (about 97% N_2 and 3% CH_4) were measured by the Cassini INMS for altitudes above 960 km [*Waite et al.*, 2005]. We also use densities shown by *Yelle et al.* [1997] for lower altitudes. Energetic particles lose energy in collisions with atmospheric neutrals via a variety of processes but mostly via ionization [cf. *Rees*, 1989]. We used stopping powers for protons or oxygen ions in nitrogen [*Paul et al.*, 1991; *Paul and Schinner*, 2001] to obtain ranges for protons and oxygen ions as functions of the initial particle energy (see Figure 2). All ions were assumed to be directed straight down and straggling was neglected. Protons penetrate deeper into the atmosphere than do oxygen ions with the same energy. Protons with energies of 1–4 MeV can produce ionospheric plasma near 500 km. The change in slope of the proton range curve near 100 keV is associated with the peak in the stopping power curve at this energy [cf. *Paul and Schinner*, 2001].

[8] Ion (and electron) production rate versus altitude profiles were calculated separately for proton and oxygen precipitation. Most atmospheric ions produced are N_2^+ (over 90%) but N^+, CH_4^+, CH_3^+... ions are also produced; our production rates should be considered to be the sum of all ion production. Ions can be produced both from direct impact ionization of a neutral (e.g., $O^+ + N_2 \rightarrow O^+ + N_2^+ + e$) and by charge transfer collisions ($O^+ + N_2 \rightarrow O + N_2^+$). The O^+ ion can be re-formed via the electron loss process ($O + N_2 \rightarrow O^+ + N_2 + e$).

[9] Basic collisional processes for H^-, H, and H^+ (proton precipitation case) and for O^-, O, O^+, and O^{++} (oxygen precipitation case) were included, and we adopted an equilibrium fraction approach for both hydrogen and oxygen beams [cf. *Rees*, 1989; *Cravens et al.*, 1995]. Due to space limitations the equilibrium fractions are not shown, but neutral oxygen dominates below about 100 keV and oxygen ions at higher energies. The fraction of O^- is about 5% for a wide range of energies. Our hydrogen beam equilibrium fractions are quite close to those shown by *Rees* [1989]. Cross sections from *Lindsay and Stebbings* [2005], *Lindsay et al.* [2004], and *Luna et al.* [2003] were adopted. For ionization by energetic neutral O and H atoms we used the corresponding O^+ cross sections and 15% of the proton ionization cross section, respectively. An $O^- + N_2$ electron loss cross section of 5×10^{-16} cm^2 was adopted.

[10] Ion production rates versus altitude were calculated by multiplying the ionization plus charge transfer cross sections with the flux of relevant charge state ions at the relevant beam energy for a given altitude and for each incident "beam" energy. The rates for all beams in a particular incident spectrum are added together at each altitude. This method neglects secondary ionization by electrons but we also estimated ion production rates from the total energy deposition rate at each altitude (i.e., from the stopping power) using a reasonable mean energy loss per ion pair (i.e., W ≈ 50 eV/ip). The ionization rates calculated this way agree rather well (≈50%) with the other ion production rates.

4. Formation of an Ionospheric Layer Below 1000 Km at Titan

[11] The calculated total (about 90% is N_2^+ and a few percent N^+) ion production rates are shown in Figure 3.

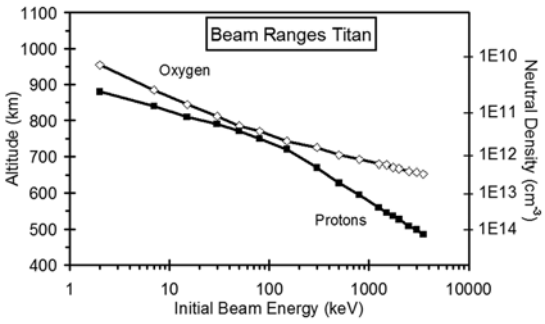

Figure 2. Ranges of oxygen ions and protons in Titan's atmosphere as functions of initial beam energy.

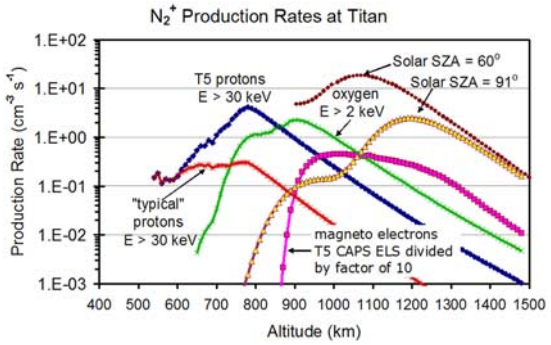

Figure 3. Ion production rate versus altitude at Titan for: energetic proton precipitation for the T5 fluxes, proton precipitation for typical conditions, energetic oxygen precipitation, ionization by solar EUV and soft x-ray radiation (for 2 solar zenith angles), and impact ionization associated with the precipitation of energetic electrons. The lower energy cutoff was set at 30 keV for the incident magnetospheric protons and at 2 keV for oxygen ions.

Methane ionization rates were not calculated but can be estimated with the methane mixing ratio (≈2–3%). Figure 3 also shows N_2^+ production rate profiles for photoionization by solar radiation and for impact ionization by precipitating magnetospheric electrons. The solar production rates are from an updated version of the *Cravens et al.* [2005] model for Ta conditions (solar zenith angle SZA ≈ 91°) and for SZA = 60°. The ionization rates for energetic electron precipitation were calculated using the methods of *Gan et al.* [1992] for T5 conditions with incident electron fluxes measured by the Cassini CAPS ELS experiment [*Coates et al.*, 2007b]. These results (discussed in a future paper) are similar to those obtained by *Agren et al.* [2007].

[12] Ion production due to solar and magnetospheric electron (energies less than 5 keV) inputs are important above 800–900 km, but cannot explain the observed high electron densities at lower altitudes (Kliore et al., submitted manuscript, 2007). The current paper demonstrates that energetic oxygen precipitation can generate significant ion production down to 650 km and that proton precipitation can generate ionization down to 480 km.

[13] Titan's ionosphere is known to be very complex chemically with a very large number of ion species [cf. *Fox and Yelle*, 1997; *Keller et al.*, 1998; *Cravens et al.*, 2006; *Vuitton et al.*, 2006]. The electron density depends on the dissociative recombination of many "terminal" ion species. Negative ions discovered in the lower ionosphere by the Cassini CAPS instrument [*Coates et al.*, 2007a] add to this chemical complexity. Nonetheless, we find a photochemical estimate of the electron density with an effective dissociative recombination rate coefficient (α): $n_e = [P/\alpha]^{1/2}$ where P is the altitude-dependent total ion production rate. We adopt $\alpha \approx 2 \times 10^{-7}$ cm^3 s^{-1} for altitudes above 1000 km and $\alpha \approx 7 \times 10^{-7}$ cm^3 s^{-1} for lower altitudes (more complex ions) with a smooth transition between them. Figure 4 shows our estimated electron density profiles for combined solar ionization and energetic proton ionization (the T5 and the "typical" cases are both shown). The electron densities generated by proton precipitation are substantial ($n_e \approx 400–1600$ cm^{-3}) near 500 km in agreement with densities measured by the Cassini radio occultation experiment (Kliore et al., submitted manuscript, 2007). The maximum in the electron density at an altitude of ≈1200 km is due to solar radiation and the peak for the T5 case near 800 km is mostly due to 30–100 keV protons. For the "typical" MIMI case, the proton flux in this energy range is much less and a distinct lower peak is not generated (only a "ledge" in the density profile).

5. Implications of Energetic Ion Precipitation for Negative Ion Creation

[14] The CAPS ELS instrument observed high abundances of negative ions [*Coates et al.*, 2007a] below 1000 km, including some very heavy aerosol-like species. No clear explanation exists at this time for these negative ions. Perhaps fast H^- and O^- ions associated with magnetospheric ion precipitation (as discussed in the current paper) can contribute to negative ion formation via charge transfer to cold thermal molecules (e.g., $O_f^- + CH_4 \rightarrow O_f + CH_3^- + H$, where "f" stands for fast). Once ionospheric species such as CH_3^- or NH_2^- are formed, the electron could transfer to higher electron affinity species (e.g., HCN).

[15] Adopting a cross section of 10^{-16} cm^2 for the initial charge transfer process, a negative ion production rate at 950 km of $P_- \approx .003$ cm^{-3} s^{-1} results. If the main negative ion nightside loss process is ion – ion recombination (rate coefficient $\alpha_- \approx 2 \times 10^{-7}$ cm^3 s^{-1}) and adopting a free electron density at 950 km of $n_e \approx 1000$ cm^{-3}, then an estimate of the negative ion density gives $n_- \approx P_-/(\alpha_- n_e) \approx 100$ cm^{-3}. This suggested scheme does not preclude other negative ion sources, such as dissociative attachment of fast electrons.

6. Summary

[16] We have demonstrated that precipitation of energetic magnetospheric ions into Titan's atmosphere has important consequences for the formation of a lower ionospheric layer (Kliore et al., submitted manuscript, 2007) as well as for the creation of negative ion species. Energy deposition by fast ions should also result in dissociation, non-ionizing electronic excitation, and neutral heating [cf. *Rees*, 1989].

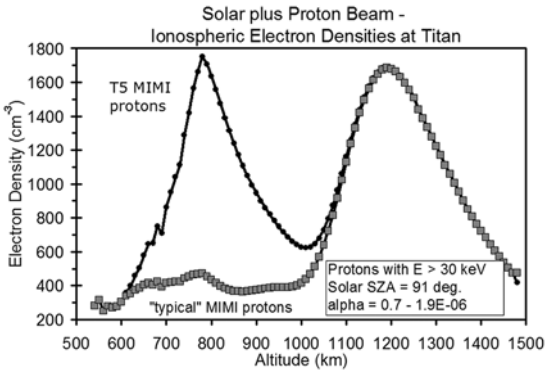

Figure 4. Electron density profiles calculated for energetic proton precipitation plus ionization by solar photons for a solar zenith angle of 91°. A simple effective dissociative recombination rate coefficient was adopted (see text).

Auroral emissions initiated by the energetic ion precipitation should also be investigated. Ion chemistry initiated by ionization and dissociation at lower altitudes can affect, via N_2 or CH_4 bond breaking, the chemistry ultimately leading to the formation of complex nitrile and hydrocarbon species [cf. *Waite et al.*, 2007; *Vuitton et al.*, 2006].

[17] **Acknowledgments.** Support from the NASA Cassini project is acknowledged (NASA grant NFP45280 via subcontract from Southwest Research Institute). Model development at the University of Kansas was also supported by NASA Planetary Atmospheres grant NNX07AF47G and by NSF grant ATM-0234271. We thank N. Jager and R. C. Dirks for computational assistance and T. Hunt-Ward for assistance with the manuscript.

References

Agren, K., et al. (2007), On magnetospheric electron impact ionization and dynamics in Titan's ram-side and polar ionosphere: A Cassini case study, *Ann. Geophys.*, *25*, 2359.

Backes, H., F. M. Neubauer, M. K. Dougherty, H. Achilleos, N. Andre, C. S. Arridge, C. Bertucci, G. H. Jones, and K. K. Khurana (2005), Titan's magnetic field signature during the first Cassini encounter, *Science*, *308*, 992.

Bird, M. K., R. Dutta-Roy, S. W. Asmar, and T. A. Rebold (1997), Detection of Titan's ionosphere from Voyager 1 radio occultation observations, *Icarus*, *130*, 426.

Coates, A. J., F. J. Crary, G. R. Lewis, D. T. Young, J. H. Waite Jr., and E. C. Sittler Jr. (2007a), Discovery of heavy negative ions in Titan's ionosphere, *Geophys. Res. Lett.*, *34*, L22103, doi:10.1029/2007GL030978.

Coates, A. J., F. J. Crary, D. T. Young, K. Szego, C. S. Arridge, Z. Bebesi, E. C. Sittler Jr., R. E. Hartle, and T. W. Hill (2007b), Ionospheric electrons in Titan's tail: Plasma structure during the Cassini T9 encounter, *Geophys. Res. Lett.*, *34*, L24S05, doi:10.1029/2007GL030919.

Cravens, T. E., E. Howell, J. H. Waite Jr., and G. R. Gladstone (1995), Auroral oxygen precipitation at Jupiter, *J. Geophys. Res.*, *100*, 17,153.

Cravens, T. E., et al. (2005), Titan's ionosphere: Model comparisons with Cassini Ta data, *Geophys. Res. Lett.*, *32*, L12108, doi:10.1029/2005GL023249.

Cravens, T. E., et al. (2006), Composition of Titan's ionosphere, *Geophys. Res. Lett.*, *33*, L07105, doi:10.1029/2005GL025575.

Fox, J. L., and R. V. Yelle (1997), Hydrocarbon ions in the ionosphere of Titan, *Geophys. Res. Lett.*, *24*, 2179.

Gan, L., C. N. Keller, and T. E. Cravens (1992), Electrons in the ionosphere of Titan, *J. Geophys. Res.*, *97*, 12,136.

Hartle, R. E., et al. (2006), Initial interpretation of Titan plasma interaction as observed by the Cassini Plasma Spectrometer: Comparisons with Voyager 1, *Planet. Space Sci.*, *54*, 1211.

Keller, C. N., V. G. Anicich, and T. E. Cravens (1998), Model of Titan's ionosphere with detailed hydrocarbon chemistry, *Planet. Space Sci.*, *46*, 1157.

Krimigis, S. M., et al. (2005), Dynamics of Saturn's magnetosphere from MIMI during Cassini's orbital insertion, *Science*, *307*, 1270.

Ledvina, S. A., and T. E. Cravens (1998), A three-dimensional MHD model of plasma flow around Titan, *Planet. Space Sci.*, *46*, 1175.

Ledvina, S. A., T. E. Cravens, and K. Kecskeméty (2005), Ion distributions in Saturn's magnetosphere near Titan, *J. Geophys. Res.*, *110*, A06211, doi:10.1029/2004JA010771.

Lindsay, B. G., and R. F. Stebbings (2005), Charge transfer cross sections for energetic neutral atom data analysis, *J. Geophys. Res.*, *110*, A12213, doi:10.1029/2005JA011298.

Lindsay, B. G., W. S. Yu, K. F. MacDonald, and R. F. Stebbings (2004), Electron capture and loss by kilo-electron-volt oxygen atoms in collisions with He, H_2, N_2, and O_2, *Phys. Rev. A*, *70*, 42,701.

Luna, H., M. Michael, M. B. Shah, R. E. Johnson, C. J. Latimer, and J. W. McConkey (2003), Dissociation of N_2 in capture and ionization collisions with fast H^+ and N^+ ions and modeling of positive ion formation in the Titan atmosphere, *J. Geophys. Res.*, *108*(E4), 5033, doi:10.1029/2002JE001950.

Ma, Y.-J., A. F. Nagy, T. E. Cravens, I. V. Sokolov, J. Clark, and K. C. Hansen (2004), 3-D global MHD model prediction for the first close flyby of Titan by Cassini, *Geophys. Res. Lett.*, *31*, L22803, doi:10.1029/2004GL021215.

Michael, M., R. E. Johnson, F. Leblanc, M. Liu, J. G. Luhmann, and V. I. Shematovich (2005), Ejection of nitrogen from Titan's atmosphere by magnetospheric ions and pick-up ions, *Icarus*, *175*, 263.

Molina-Cuberos, G. J., et al. (2001), Ionosphere layer induced by meteoric ionization in Titan's atmosphere, *Planet. Space Sci.*, *49*, 143.

Neubauer, F. M., D. A. Gurnett, J. D. Scudder, and R. E. Hartle (1984), Titan's magnetospheric interaction, in *Saturn*, edited T. Gehrels and M. S. Matthews, p. 760, Univ. of Ariz. Press, Tucson.

Paul, H., and A. Schinner (2001), An empirical approach to the stopping power of solids and gases for ions from Li to Ar, *Nucl. Instrum. Methods Phys. Res., Sect. B*, *179*, 299.

Paul, H., D. Semrad, and A. Seilinger (1991), Reference stopping cross sections for hydrogen and helium ions in selected elements, *Nucl. Instrum. Methods Phys. Res., Sect. B*, *61*, 261.

Rees, M. H. (1989), *Physics and Chemistry of the Upper Atmosphere*, Cambridge Univ. Press, Cambridge, U. K.

Vuitton, V., R. V. Yelle, and V. G. Anicich (2006), The nitrogen chemistry of Titan's upper atmosphere revealed, *Astrophys. J.*, *647*, L175.

Wahlund, J.-E., et al. (2005), Cassini measurements of cold plasma in the ionosphere of Titan, *Science*, *308*, 986.

Waite, J. H., Jr., et al. (2005), Ion Neutral Mass Spectrometer (INMS) results from the first flyby of Titan, *Science*, *308*, 982.

Waite, J. H., D. T. Young, T. E. Cravens, A. J. Coates, F. J. Crary, B. Magee, and J. Westlake (2007), The process of tholin formation in Titan's upper atmosphere, *Science*, *316*, 870.

Yelle, R. V., D. F. Strobel, E. Lellouch, and D. Gautier (1997), The Yelle Titan atmosphere engineering models, in *Huygens: Science, Payload and Mission*, *Proceedings of an ESA Conference*, edited by A. Wilson, p. 243, ESA Publ., Noordwijk, Netherlands.

Young, D. T., et al. (2005), Composition and dynamics of plasma in Saturn's magnetosphere, *Science*, *307*, 1262.

T. E. Cravens and I. P. Robertson, Department of Physics and Astronomy, University of Kansas, Lawrence, KS 66045, USA. (cravens@ku.edu)

S. M. Krimigis and D. Mitchell, Applied Physics Laboratory, Johns Hopkins University, 11100 Johns Hopkins Road, Laurel, MD 20723, USA.

S. A. Ledvina, Space Science Laboratory, University of California, Berkeley, 7 Gauss Way, Berkeley, CA 94720, USA.

J. H. Waite Jr., Southwest Research Institute, 6220 Culebra Road, San Antonio, TX 78228-0510, USA.